Cell Partitioning Antenna System Performance in Multi-User Scenarios for mmWave Communications

Citation for the original published paper (version of record):
Bressner, T., Elsakka, A., Farsaei, A. et al (2021). Cell Partitioning Antenna System Performance in Multi-User Scenarios for mmWave Communications. IEEE Access, 9: 127141-127149.
http://dx.doi.org/10.1109/ACCESS.2021.3110939

IEEE Access
Multidisciplinary ⋮ Rapid Review ⋮ Open Access Journal

Received July 25, 2021, accepted August 28, 2021, date of publication September 7, 2021, date of current version September 20, 2021.

Digital Object Identifier 10.1109/ACCESS.2021.3110939

Cell Partitioning Antenna System Performance in Multi-User Scenarios for mmWave Communications

THOMAS A. H. BRESSNER[1], AMR ELSAKKA[1], AMIRASHKAN FARSAEI[2], MARTIN N. JOHANSSON[3], (Senior Member, IEEE), OLEG A. IUPIKOV[4], (Member, IEEE), ROB MAASKANT[4], (Senior Member, IEEE), A. BART SMOLDERS[1], (Senior Member, IEEE), AND ULF JOHANNSEN[1], (Member, IEEE)

[1]Electromagnetics Group, Department of Electrical Engineering, Eindhoven University of Technology, 5612 AJ Eindhoven, The Netherlands
[2]Signal Processing Systems, Department of Electrical Engineering, Eindhoven University of Technology, 5612 AJ Eindhoven, The Netherlands
[3]Ericsson Research, Ericsson AB, 417 56 Gothenburg, Sweden
[4]Antenna Systems Group, Department of Electrical Engineering, Chalmers University of Technology, 412 96 Gothenburg, Sweden

Corresponding authors: Thomas A. H. Bressner (t.a.h.bressner@tue.nl) and Amr Elsakka (a.a.h.m.elsakka@tue.nl)

This work was supported by the European Union's Horizon 2020 Research and Innovation Programme under Marie Sklodowska-Curie Grant 721732.

ABSTRACT Fixed-beam, high-gain antenna systems can be used for a finer partitioning of the currently used cell-sectoring. This partitioning has the benefit of reducing the number of users seen per antenna beam, which reduces interference. Furthermore, the high antenna gain allows for a high effective isotropic radiated power while keeping the transmit power low. In this paper, we study the performance of such a fixed-beam, high gain antenna system design for millimeter-wave mobile communications. The antenna system is designed to keep the inter-sector interference in a multi-site scenario low. The performance is analyzed for single- and multi-user environments. In single-input single-output mode, the 50th percentile of the signal-to-interference-plus-noise ratio lies between 12.5 dB to 39.7 dB if 3 to 0 interferers are present, respectively. For multiple-input multiple-output transmission using zero-forcing, the signal-to-interference-plus-noise ratio increases and the 50th percentile ranges from 36.1 dB to 43.3 dB if 3 to 0 interferes are present, respectively. By using maximum ratio transmission, the best performance is achieved with no interferers present, while a plunge in performance is observed with interferers. Furthermore, the study revealed that the narrow beam antenna system can also provide a clear signal separation for small spatial separations. In the given example, the signal-to-interference-plus-noise ratio is larger than 32.1 dB with 11 active antenna elements, where 2.8 meters separate the users. Hence, the paper shows that the cell-partitioning antenna systems provide coverage in the desired area while keeping the inter-sector interference low, and the considered transmission techniques can be used for situation optimized mobile communication links.

INDEX TERMS 5G mobile communication, base stations, antenna array, aperture antennas, MIMO, SISO.

I. INTRODUCTION

For the fifth-generation (5G) of telecommunications, it was predicted in [1] that there are about 220 million 5G subscriptions by the end of 2020. By the end of 2026, this number will rise up to 3.5 billion. Hence, interference becomes more and more significant and needs to be addressed for future mobile communication systems. One possible implication can be the move from larger mobile communications cells to smaller cells. Smaller cells have multiple benefits due to the shorter distance between base stations (BSs) and user equipments (UEs), like smartphone devices. For instance, propagation loss becomes less limiting, and a lower number of UEs has to be served per BS. However, smaller cell sizes come along with a higher number of sites, e.g. cellular radio towers, that are needed in an area, which will increase the network's deployment cost significantly.

One way to overcome the need for more sites is to partition mobile communication cell-sectors in smaller regions. The partitioning can be seen as an extension of the currently

The associate editor coordinating the review of this manuscript and approving it for publication was Masood Ur-Rehman.

used 60° and 120° sectors (cell-sectoring). While low-gain antennas are used for near regions, high-gain antennas are used to partition regions in far distances. Therefore, with the same number of sites, much smaller regions can be defined and covered.

Due to the distinction of near and far regions, and antennas with different antenna gains, it is possible to communicate to UEs at any distance while keeping the transmit power low. That is possible because a high effective isotropic radiated power (EIRP) is, to a large extent, achieved by the antenna gain. Therefore, multiple research groups are developing multi-beam, high-gain antenna systems. The highest flexibility has the full digital massive multiple-input-multiple-output (MIMO) approach [2] that utilizes a large number of antenna elements, where each element is connected to a radio-frequency (RF) chain to allow full control. However, such a system suffers currently from hardware cost and its power consumption. These problems are mitigated by the hybrid massive MIMO approach [3], where phased controlled sub-arrays are introduced to lower the number of RF chains without sacrificing much of its flexibility. Another approach to reducing the hardware complexity is to introduce focusing components such as lenses and reflectors. An example of such a system is given in [4], where phased-array fed reflectors are studied. Due to the use of a reflector, a lower number of antenna elements is needed to achieve a certain antenna gain, which comes at the cost of a limited field of view.

A general downside of high-gain antenna systems can be the decreased beamwidth. In [5], it is shown that the reduced beamwidth restricts the angular spread of the received signals, which affects the channel covariance matrix's eigenvalues, resulting in a MIMO performance degradation. Therefore, in [6] it was studied how the decrease of the beamwidth influences the performance of fixed-beam antenna systems, which uses high-gain antenna elements to partition a sector in smaller areas. The outcome shows that the beam diversity, due to cell-partitioning, lowers the correlation between the channels observed by each element. Hence, fixed-beam, high-gain antenna systems benefit from low correlation and a high gain per beam.

Driven by this outcome, we have designed a multi-lens-horn (MLH) antenna system, displayed in Fig. 1, for a fixed-beam scenario and tested it in this study. This lens-horn antenna element approach benefits that each element provides a highly directive beam without analog beamforming. Hence, no complex feeding structure, phase shifters, or regular calibration is needed compared to the hybrid massive MIMO, and phased-array fed reflector approaches. On the other hand, the developed system has less degrees of freedom when it comes to beam optimization, and it is bounded by the radiation patterns and orientations of the single antenna elements in the fixed-beam scenario. In particular, the reduced beam overlap could lead to poor MIMO performance since fewer elements can contribute to the overall pattern. Hence, this paper shows the system performance in single-input single-output (SISO) and MIMO mode.

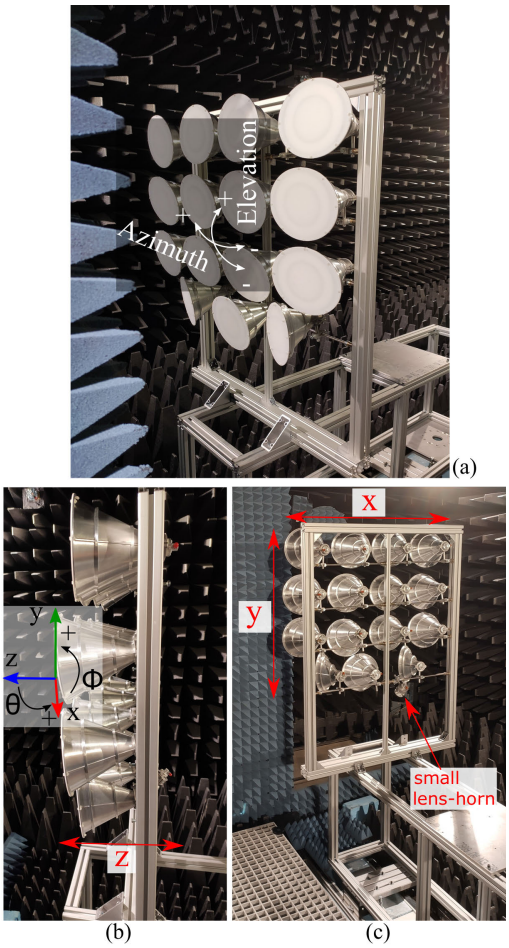

FIGURE 1. Mounted MLH-antenna system with the dimensions of 82 cm, 76.5 cm, 38 cm (x, y, z). (a), (b) and (c) show the front, side and back views, respectively.

The antenna under test is a high-gain dual-polarized antenna system designed for a 60° unit sector using 16 antenna elements where each is fed with a low TX power of 26 dBm. The system is analyzed in terms of achievable signal-to-noise ratio (SNR) and signal-to-interference-plus-noise ratio (SINR) for single and multi-user cases. This study is performed with different transmission modes, such as SISO mode and MIMO mode using zero-forcing (ZF) and maximum ratio transmission (MRT). While for SISO mode, each UE is served by a single beam, multiple elements are utilized in ZF and MRT to optimize for low interference and high signal strength, respectively.

In Section II, the system under test is summarized, and the considered scenario is described. In Section III, the simulation results for coverage, multi-site interference, SNR for single-user, and SINR for multi-user cases are presented. In Section IV the conclusion is drawn.

II. SYSTEM AND SCENARIO DESCRIPTION

This study evaluates the downlink performance of a cell partitioning antenna system that is developed by the Eindhoven University of Technology. The antenna system consists of 16 compact lens-horn antennas with total size of 82 cm,

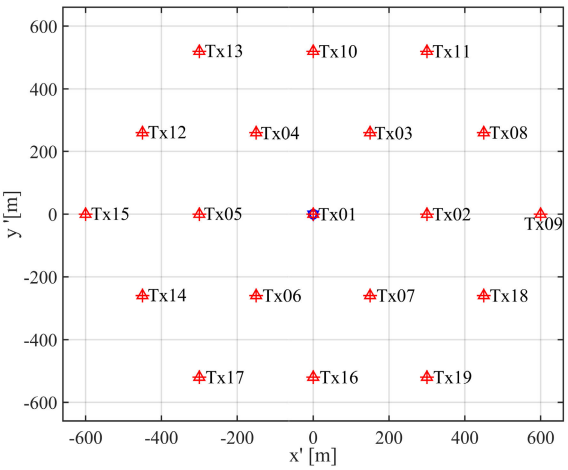

FIGURE 2. Constellation of the 19 sites scenario.

TABLE 1. Scenario parameters.

Description	Parameters
ISD	300 m
Sector opening	60°
H_{BS}	10 m
H_{UE} [m]	1.5 m
f_{c}	28 GHz
Channel bandwidth, B	400 MHz[1]
Ambient Temperature (T)	290 K
Transmit power, P_{TX}	26 dBm[2]
UE distribution	Randomly and uniformly distributed

76.5 cm, 38 cm (x, y, z) shown in Fig. 1. For this study, the simulation parameters shown in Table 1 are considered. In total, there are 19 sites with an inter-site distance (ISD) of 300 m, where each site has six sectors. Since the MLH-antenna system is designed as a unit sector, six of them can be used to provide 360° coverage. The location of the different sites is shown in Fig. 2.

The performance evaluation of the MLH-antenna system is studied by loading the radiation characteristics obtained by full-wave simulations using CST Microwave Studio® , into a MATLAB system simulation. For the coverage analysis, the radio channel generator QuaDRiGa [7] is used to obtain information about a multi-site scenario in Section III-A. For the performance analysis of the MLH-antenna system in a single sector, an in-house developed toolbox for Matlab is used. The developed Matlab implementation is based on a high-level system model for a communications system that includes a base station antenna (BSA) system, a free-space propagation channel, and user equipment (UE) antennas. This system model is explained in detail in this Section, and the performance study results are given in Section III-B.

A. SYSTEM NETWORK MODEL

The system model in Fig. 3 represents the mobile communication system in downlink scenario. At the transmitter side,

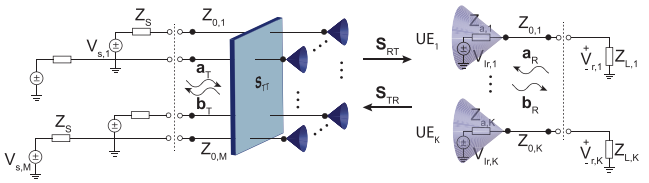

FIGURE 3. System network model representation.

the m^{th} base station antenna (BSA) is excited by a peak voltage $V_{\text{s},m}$ with a matched port impedance (Z_{s}) to both, the characteristic impedance $Z_{0,m}$ and the antenna impedance, where $m = 1, 2, \ldots, M$. While at the receiver side, an incident plane wave induces an open-circuit (Thevenin) voltage $V_{\text{Ir},k}$ on the k^{th} UE antenna terminals, where $k = 1, 2, \ldots, K$. Each UE has an isolated antenna impedance of $Z_{\text{a},k}$ that is matched to both, the characteristic impedance $Z_{0,k}$, and a receiver load impedance of $Z_{\text{L},k}$ ($Z_{\text{a},k} = Z_{0,k} = Z_{\text{L},k} = 50\Omega$). The block-matrix partitioned S-parameter equation for this system is:

$$\begin{bmatrix} \mathbf{b}_{\text{T}} \\ \mathbf{b}_{\text{R}} \end{bmatrix} = \begin{bmatrix} \mathbf{S}_{\text{TT}} & \mathbf{S}_{\text{TR}} \\ \mathbf{S}_{\text{RT}} & \mathbf{S}_{\text{RR}} \end{bmatrix} \begin{bmatrix} \mathbf{a}_{\text{T}} \\ \mathbf{a}_{\text{R}} \end{bmatrix} \tag{1}$$

where the incident power waves ($\mathbf{a}_{\text{T}}$ and $\mathbf{a}_{\text{R}}$) and backward power waves ($\mathbf{b}_{\text{T}}$ and $\mathbf{b}_{\text{R}}$) are defined as in [10]. The sizes of the above mentioned vectors and matrices in (1) can be defined as follows: $\mathbf{a}_{\text{T}} \in \mathbb{C}^{M\times 1}$, and $\mathbf{a}_{\text{R}} \in \mathbb{C}^{K\times 1}$, while $\mathbf{b}_{\text{T}} \in \mathbb{C}^{M\times 1}$, and $\mathbf{b}_{\text{R}} \in \mathbb{C}^{K\times 1}$. The BSAs inter-mutual coupling and input reflection coefficients are modeled in $\mathbf{S}_{\text{TT}} \in \mathbb{C}^{M\times M}$, while for the UEs it is modeled as $\mathbf{S}_{\text{RR}} \in \mathbb{C}^{K\times K}$. Since $\lambda \simeq 1$ cm at 28 GHz, the mutual coupling between UEs is ignored, and hence, $\mathbf{S}_{\text{RR}}$ is a diagonal matrix that accounts for the UE equivalent source models shown in Fig. 3. The uplink channel matrix is modeled as $\mathbf{S}_{\text{TR}} \in \mathbb{C}^{M\times K}$, while the downlink channel matrix is modeled as $\mathbf{S}_{\text{RT}} \in \mathbb{C}^{K\times M}$.

From (1) the elements of the downlink channel matrix s_{RT} can be calculated as,

$$s_{\text{RT}} = \left.\frac{b_{\text{R},k}}{a_{\text{T},m}}\right|_{a_{\text{R},k}=0} = \frac{1}{2}\left(\sqrt{\Re \text{Z}_{\text{a},k}}\right)^{-1} V_{\text{Ir},k,m}, \tag{2}$$

where, a_{T} is assumed to be $1[\sqrt{\text{Watt}}]$. The received induced voltage $\mathbf{V}_{\text{Ir},k,m}$ for user k can be calculated as in [11, pp. 61] using the antenna reciprocity theorem and the reaction concept. Based on that, assuming an isotropic radiators at the UEs each of which matches the incident plane wave polarization vector, the elements of the channel matrix $\mathbf{S}_{\text{RT}}$ can be written as,

$$s_{\text{RT},m,k} = \frac{1}{2\sqrt{Z_{\text{a},k}}} \frac{-2j\lambda}{\eta_0 I_{\text{at},k}} G_{k,\text{co}}(\hat{r}) G_{m,\text{co}}(-\hat{r}) \frac{1}{r_k} e^{-jkr_k}, \tag{3}$$

where r_k is the distance between the BSA and the UE phase reference points, λ is the free-space wavelength, and η_0 is the free-space wave impedance. $G_{m,\text{co}}(-\hat{r})$ and $G_{k,\text{co}}(\hat{r})$ are the co-components of the transmit and receive antennas' far-field functions respectively. A far-field function $\mathbf{G}(\hat{r})$ can be obtained from the radiated E-field $\mathbf{E}_{\text{rad}}(r, \theta, \phi)$ through,

$$\mathbf{G}(\hat{r}) = \mathbf{E}_{\text{rad}}(r, \theta, \phi) r e^{jkr}. \tag{4}$$

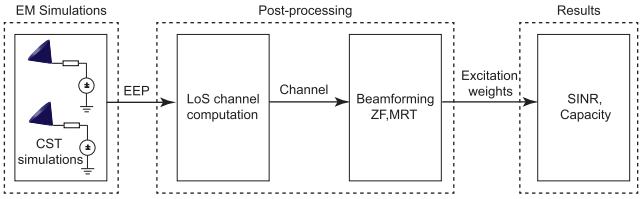

FIGURE 4. Performance characterization workflow.

Finally, $I_{\text{at},k}$ is the peak current that is used to excite the UE antenna yielding the UE far-field function $\mathbf{G}_k(\hat{r})$.

B. PERFORMANCE CHARACTERIZATION WORKFLOW

The performance characterization workflow comprises three steps as shown in Fig. 4. In the first step, the embedded element patterns (EEPs) of the lens-horns are obtained using CST Microwave studio®. The second step is the post-processing, where the line-of-sight (LoS) channel is computed as in (3), then beamforming is done to obtain the excitation weights. The excitation weights $\mathbf{W} \in \mathbb{C}^{M\times K}$ are obtained by using either the MRT beamformer,

$$\mathbf{W} = \mathbf{S}_{\text{RT}}^{\text{H}}, \tag{5}$$

or using the ZF beamformer,

$$\mathbf{W} = \mathbf{S}_{\text{RT}}^{\text{H}}(\mathbf{S}_{\text{RT}}\mathbf{S}_{\text{RT}}^{\text{H}})^{-1}, \tag{6}$$

where the H indicates the matrix Hermitian. The normalized excitation weights vector for each user $\tilde{\mathbf{w}}_k$ is obtained by,

$$\tilde{\mathbf{w}}_k = \begin{cases} \dfrac{\mathbf{w}_k}{\sqrt{\max\limits_m\left(\sum\limits_{k'=1}^{K}|\mathbf{W}_{m,k'}|^2\right)}} & \exists m\left(\sum\limits_{k'=1}^{K}\left|\dfrac{w_{m,k'}}{\max(|\mathbf{w}_{k'}|)}\right|^2\right) > 1 \\ \dfrac{\mathbf{w}_k}{\max(|\mathbf{w}_k|)} & O.W. \end{cases} \tag{7}$$

This way, the per-antenna power constraint is ensured since the sum of weights from all active users on a single element cannot exceed the value of 1. Finally, in the third step, the SINR can be calculated as,

$$\text{SINR}_k = \frac{|\mathbf{S}_{\text{RT},k}\tilde{\mathbf{w}}_k|^2\, P_{\text{TX}}}{\sum\limits_{j=1,j\neq k}^{K}|\mathbf{S}_{\text{RT},j}\tilde{\mathbf{w}}_j|^2 P_{\text{TX}} + N} \tag{8}$$

where N is the receiver noise power and it can be calculated by,

$$N = KTB, \tag{9}$$

where B is the Rx bandwidth, K is the Boltzmann's constant and T is the ambient temperature (290 Kelvin).

III. INTERFERENCE AND COVERAGE ANALYSIS

A. MULTI-SITE SCENARIO COVERAGE

The MLH-antenna system is originally designed to provide coverage within the desired sector while keeping the overlap between beams and adjacent sectors low. Therefore, the coverage lies above 95% of the defined sector for vertical and horizontal polarization in the n257 band (26.5-29.5 GHz).

Now, it is studied how the MLH-antenna system performs in a multi-site scenario with the constellation given in Fig. 2. For good performance, it is expected that the inside of a sector is served by the corresponding MLH-antenna system, while the MLH-antenna system should have low interference with adjacent sectors and sites. In Fig. 5, multiple UEs are distributed over the entire multi-site scenario. For each UE, the received signal strength is compared between every possible MLH-antenna system. Based on the signal strength, each UE is assigned to the MLH-antenna system that provides the strongest signal to the specific UE. This scheme is a common way how UEs are assigned to a BS. Note that only the inner seven sectors of the multi-site scenario are plotted for better visibility, and a color-coding is used to visualize the assigned sector. The plot shows clear sectors of triangular shapes due to the MLH-antenna system characteristics together with the applied free-space propagation model. There are only a few outliers seen near the edges. These exceptions are reasonable since, at the overlap of two or more beams, each beam's signal strength is the same.

For better visualization, Fig, 6 shows a close up on sector number one. Note that the color-coding is kept the same as in Fig. 5. The zoomed-in plot reveals that the strongest signals that originate from other sectors are sectors 2, 6, 10, 17, and 39. While sectors 2 and 6 are adjacent, the others are pointing towards sector 1. Particularly, sector 10 provides the strongest signal near the edge. This impact is mainly due to the spread of the beams, which is visible in Fig. 7 showing a heat map of the achievable SNR. The plot shows clearly, how the beamwidth and pointing direction are linked to the SNR coverage. It is also possible to identify all 16 beams clearly since there is only a small overlap between them. Furthermore, we see that some spots show distinct lower SNR values. This becomes significant near the BS, where some other sectors provide a strong signal, shown in Fig. 6. In general, such a problem can be optimized to a certain extent by adjusting each antenna element's pointing direction. Another way would be to assign different frequency spectra to potential interferers as sectors 2, 6, 10, 17, and 39, eliminating the inter-sector interference.

B. SINGLE- AND MULTI-USER PERFORMANCE STUDY

In the following, the beam orientation is kept the same, and the system's performance is analyzed for intra-sector interference for sector 1. Furthermore, a practical excitation limit is set where the antenna elements with relative amplitude weights below −15 dB are switched off. This is tested for SISO and MIMO mode transmission.

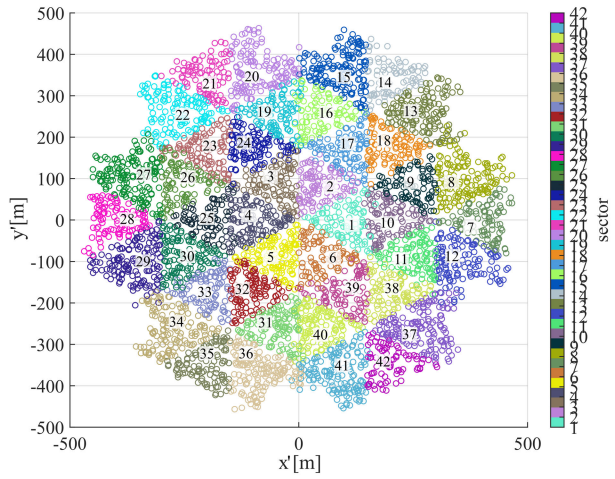

FIGURE 5. Serving sectors based on signal strength, displayed for the seven inner sites showing 42 sectors.

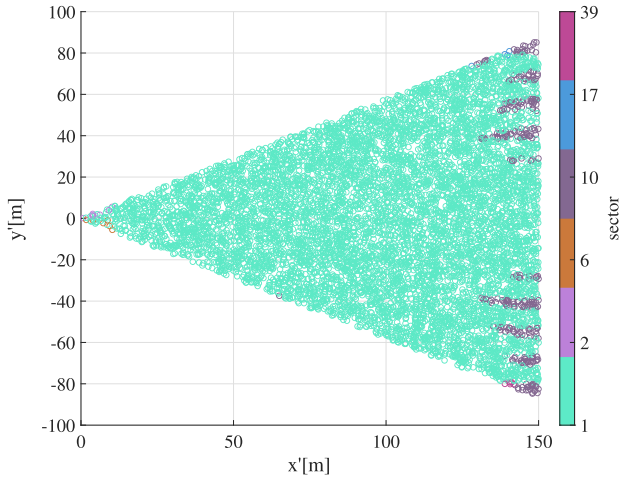

FIGURE 6. Serving sectors based on signal strength, shown for single sector.

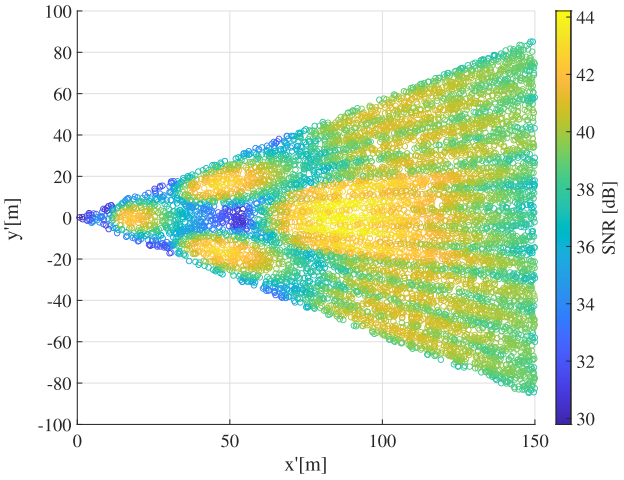

FIGURE 7. Heat map plot of the achievable SNR for SISO mode communications for a single-sector scenario.

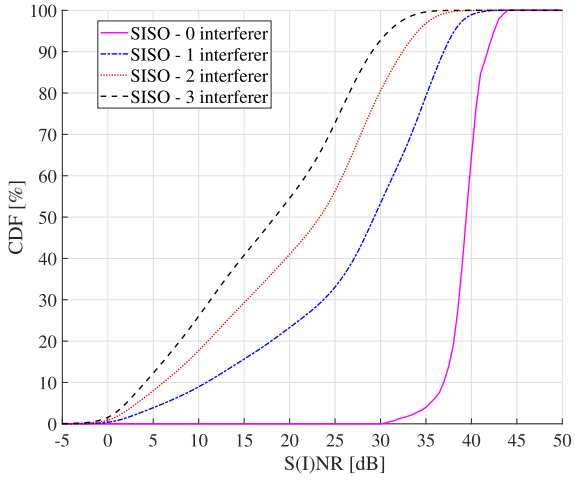

FIGURE 8. CDF plot of the achievable S(I)NR for SISO mode communications for a single-sector scenario if 0, 1, 2, and 3 interferers are present.

1) SISO MODE

The heat map of the achievable SNR shown in Fig. 7 reveals that the SNR can be expected to be between 30 dB and 45 dB in SISO mode if a single UE is active at the same time instant. However, due to the beam isolation, it is possible to serve multiple UEs simultaneously without suffering much from interference. The SISO mode performance is simulated for 0, 1, 2, and 3 interferer present, with the constraint that the interferer cannot be in the serving beam. The results of the study is plotted in Fig. 8 and the 10^{th}, 50^{th}, and 90^{th} percentiles are listed in Table 2. In the case that there is only a single UE present in the sector, the achieved SNR values lie as expected between 29 and 45 dB. By introducing additional active UEs in the sector, the SINR drops successively for every added UE. The most significant change is visible around the 10^{th} percentile, which are the cases where the served UE is near the edge of its serving beam while an interferer is also located near the edge region. However, in the more common case, represented by the 50^{th} percentile, the S(I)NR ranges from 12.5 dB to 39.7 dB if 3 to 0 interferers are present, respectively. Furthermore, the good beam isolation allows to achieve 27.6 dB in the best case (90^{th} percentile) if three interferers are present.

2) MIMO MODE USING ZF AND MRT

So far, we have considered using each element of the MLH-antenna system separately (SISO mode). However, the MLH-antenna system can also be used as a MIMO system since each of the 16 antennas can be controlled separately, and the radiation beams slightly overlap. Hence, it is possible to apply beamforming techniques as ZF and MRT. In Fig. 9 the obtained statistics for the ZF and MRT are displayed for 1, 2, and 3 interferers. In the case of MRT, also 0 interferers (MRT SNR) are considered.

Comparing the MRT SNR to SISO SNR, higher SNR values are expected if MRT is applied due to the utilization of multiple antenna elements. It can be seen that this is true in Table 2 by comparing the third and fourth column that shows the obtained 10^{th}, 50^{th}, and 90^{th} percentiles for the different numbers of interferers. At the 10^{th} and 90^{th} percentile,

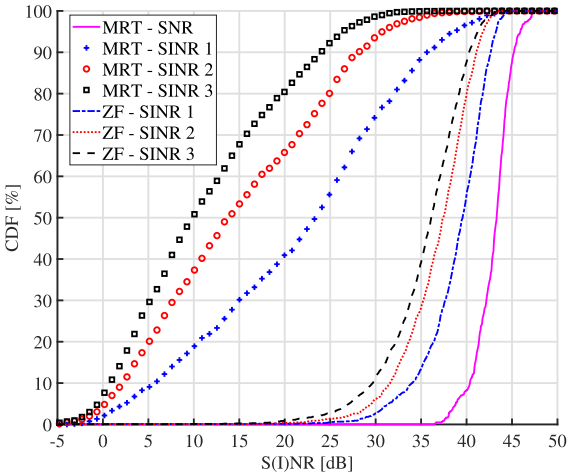

FIGURE 9. Obtained S(I)NR statistics applying ZF and MRT for 0, 1, 2, and 3 interferer present.

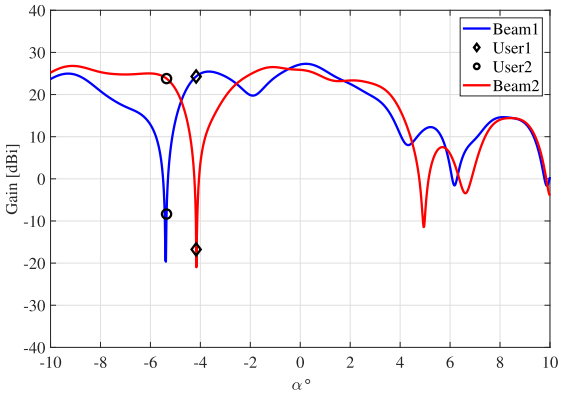

FIGURE 10. Zero forcing applied for two users with a 2.8 meter spacing, where the blue line shows the radiation beam for user 1 and the red line depicts the radiation pattern for user 2. The user locations with respect to α in degree is indicated by a circle and diamond.

TABLE 2. SISO and MIMO performance shown for 10^{th}, 50^{th}, and 90^{th} percentiles for the considered transmission techniques.

Interferer	Percentile	SISO S(I)NR	MRT S(I)NR	ZF SINR
0	10^{th}	36.7 dB	40.4 dB	-
0	50^{th}	39.7 dB	43.3 dB	-
0	90^{th}	42.4 dB	45.2 dB	-
1	10^{th}	3.8 dB	5.6 dB	34 dB
1	50^{th}	26.8 dB	23.4 dB	39.6 dB
1	90^{th}	36.2 dB	35.7 dB	42.7 dB
2	10^{th}	0.5 dB	2.1 dB	31.6 dB
2	50^{th}	18.5 dB	13.7 dB	37.4 dB
2	90^{th}	31.1 dB	28.1 dB	41.1 dB
3	10^{th}	-0.9 dB	0.8 dB	29.6 dB
3	50^{th}	12.5 dB	9.8 dB	36.1 dB
3	90^{th}	27.6 dB	24 dB	40.3 dB

the SNR is increased by 3.7 dB and 2.8 dB, respectively. The most significant increase is seen at the borders where two or more adjacent beams intersect. However, this advantage is not given if there are multiple active UEs. This is because MRT maximizes the transmit power to all active users while not actively suppressing the interference. Hence, the use of MRT causes more interference, and the SINR drops. Therefore,

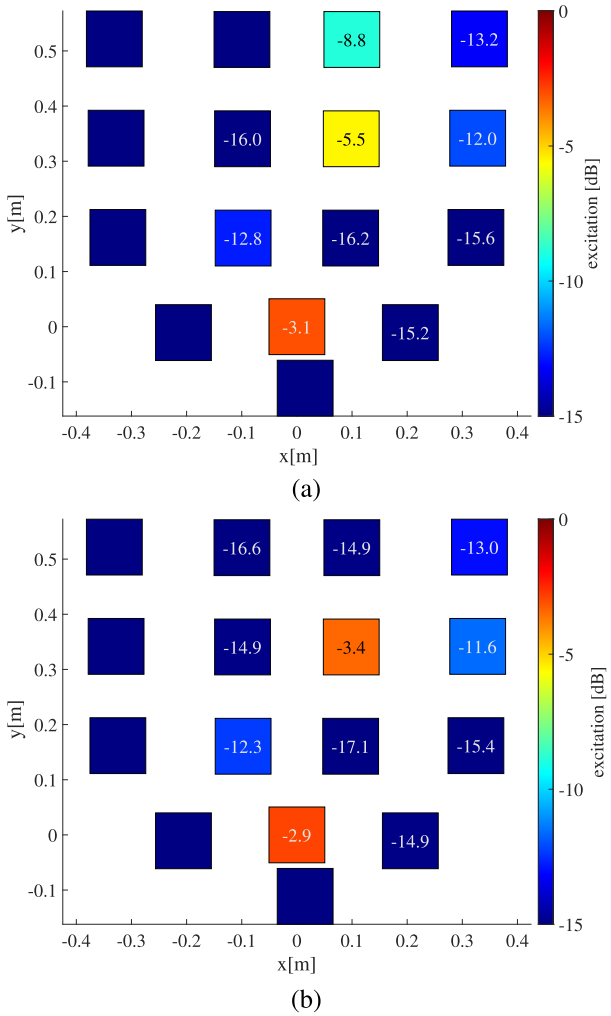

FIGURE 11. Excitation values given in dB for (a) user 1 and (b) user 2 to generate the radiation beams shown in Fig. 10. Each tile represents one element and are in the constellation of the MLH system shown in Fig. 1.

with the increasing number of interferers, the SISO mode performs better.

In contrast, ZF significantly outperforms SISO operation. The ZF performs for 1, 2, and 3 interferers similarly to the SISO mode without interference. For instance, with three interferers present, the ZF still provides an SINR of 29.6 dB to 40.3 dB, which is significantly higher compared to SISO mode and MRT. Therefore, in the case of having multiple interferers, the use of ZF is beneficial to the system performance.

Finally, we have picked two examples from the complete set of simulations performed to obtain the statistics. The intention is to show how well the signals are separated and how many antenna elements have to be active for two users that are close together and far apart. The signal separation for these two cases is of interest since the narrow beams have only a slight overlap of the observed areas per beam. Hence, the number of contributing antenna elements to the beam is reduced, resulting in a likely worse signal separation for closely spaced users.

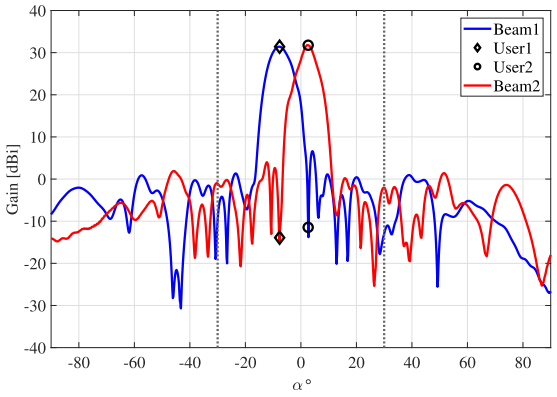

FIGURE 12. Zero forcing applied for two UEs with a 30 meter spacing, where the blue line shows the radiation beam of user 1 and the red line depicts the radiation pattern of user 2. The user locations with respect to α in degree is indicated by a circle and diamond.

For the closely placed users, we have selected two users with a 2.8 meters spacing, where UE1 is at the location (89.6 m; 103.7 m) and UE2 at (87.6 m; 105.7 m) given in the form of $(x'; y')$ in meters. In the second case, the users are 30 meters apart, where UE1 is at the location (71.5 m; 93.7 m) and UE2 at (69.5 m; 63.4 m). This part of the study is only performed for ZF due to the low performance of MRT if interferers are present.

The quality of the user separation is demonstrated, where for each scenario, we use the far-field cut that passes through the user locations on the far-field grid since the UEs are located on different elevation scan angles. The principal plane's far-field cuts will not allow this demonstration. We get such cuts as follows; first, the far-field grid in a spherical coordinate system is converted to a True-view grid with Azimuth and Elevation directions. The Azimuth and Elevation coordinates are obtained as in [12, pp. 364] to be,

$$\text{Azimuth} = -\theta \cos\phi, \tag{10}$$

$$\text{Elevation} = \theta \sin\phi, \tag{11}$$

and their directions are indicated in Fig. 1. Then, the UE locations are determined in Azimuth and Elevation coordinates knowing the user physical locations with respect to the antenna coordinate system. Finally, the required cut is extracted, and the label of the X-axis α in Fig. 10 and Fig. 12 is defined to be,

$$\alpha = \sqrt{\text{Azimuth}^2 + \text{Elevation}^2}. \tag{12}$$

In Fig. 10 the resulting radiation pattern is shown for the two UEs with 2.8 meters spacing, and the exact position with respect to the beam is marked in the graph. The blue line depicts the radiation pattern for UE1 and the red line for UE2. It can be seen that in this particular case, an SINR for UE1 is 41 dB, and for UE2, an SINR of 32.1 dB. Therefore, although the two UEs are only separated by 2.8 meters, a good signal separation is achieved. The excitation values are displayed per antenna element in Fig. 11, where each tile represents

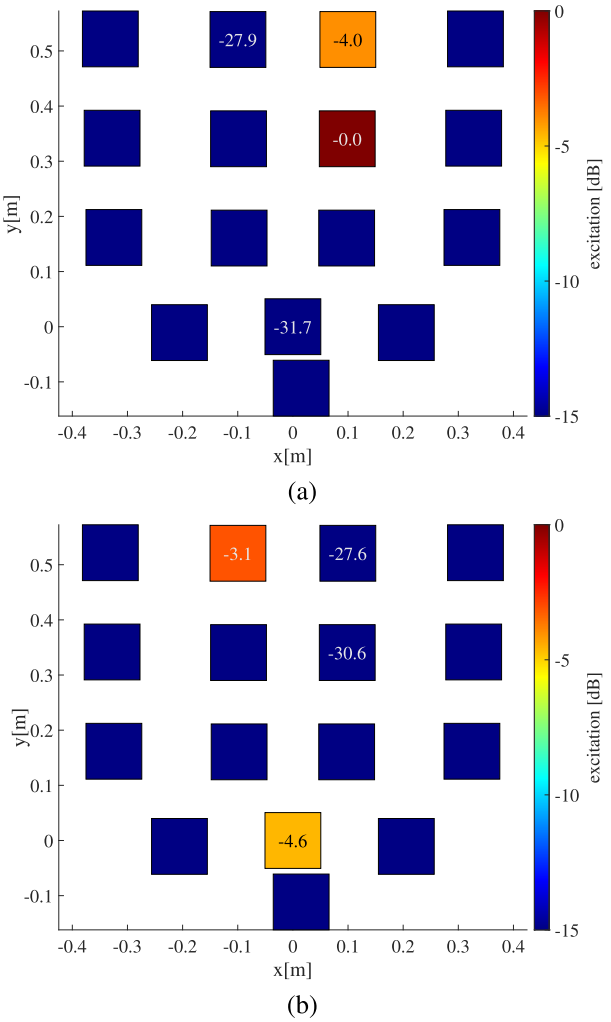

FIGURE 13. Excitation values given in dB for (a) user 1 and (b) user 2 to generate the radiation beams shown in Fig. 12. Each tile represents one element and are in the constellation of the MLH system shown in Fig. 1.

one antenna element with respect to the constellation of the MLH-antenna system shown Fig. 1. We can see that the beams are generated with 10 and 11 active elements for UE1 and UE2, respectively. While 2 to 3 elements significantly contribute, the other antenna elements still contribute slightly to the beam shape.

In Fig. 12 the resulting radiation pattern is shown for the two UEs that are separated by 30 meters. The blue line depicts the radiation pattern for UE1 and the red line for UE2. As expected, the ZF algorithm also provides for UEs with a large spatial separation, a high SINR of 45.3 dB and 43.2 dB for UE1 and UE2, respectively. However, a significant difference can be seen in the number of active elements shown in Fig. 13. We see that the number of active elements reduces, which is still enough to separate the two signals clearly. In general, we have observed that the number of active antenna elements depends on the UEs' position with respect to the interferers and the antenna beams. Hence, not all antenna elements can contribute to the signal that a UE receives. Still, a clear signal separation can be provided for

closely spaced UEs, which demonstrated by this example, and it is reflected in the high SINR of the 10th percentile that is observed in statistics.

IV. CONCLUSION

We have shown the capabilities of a cell partitioning high-gain multi-lens-horn antenna system that uses only 26 dBm transmit power per antenna element. The performance is analyzed in terms of coverage in a multi-site scenario and the S(I)NR for ZF and MRT beamforming and SISO communication. The low influence by adjacent sectors and sites is achieved by an optimized antenna orientation of the high-gain antenna beams. Furthermore, the MLH-antenna system showed that depending on the number and position of the interferers, SISO, ZF, and MRT mode can be beneficial. MRT provides the highest SNR, e.g. 45.2 dB (90th percentile), but exhibits, in general, the worst performance in the presence of interferers. With the presence of interferer, the use of ZF is advantageous, e.g. with three interferers present, the achieved SINR (90th percentile) is 16.3 dB and 12.7 dB higher compared to MRT and SISO mode, respectively.

We can conclude that the MLH-antenna system can be used in SISO and MIMO mode, where the highest SINR is achieved with ZF. In either case, the highly-directional beams provide signals with high signal strength while keeping the TX power low.

ACKNOWLEDGMENT

(Thomas A.H. Bressner and Amr Elsakka contributed equally to this work.)

REFERENCES

[1] W. Obile, "Ericsson mobility report," Ericsson AB, Stockholm, Sweden, Tech. Rep. EAB-20:009174, Nov. 2020.
[2] E. G. Larsson, O. Edfors, F. Tufvesson, and T. L. Marzetta, "Massive MIMO for next generation wireless systems," *IEEE Commun. Mag.*, vol. 52, no. 2, pp. 186–195, Feb. 2014.
[3] R. M. Vaghefi, G. Miranda, R. Srirambhatla, G. Marzin, C. Ng, F. Fayazbakhsh, S. Tarigopula, R. C. Palat, and M. Banu, "First commercial hybrid massive MIMO system for sub-6Hz bands," in *Proc. IEEE 5G World Forum (5GWF)*, Jul. 2018, pp. 357–362.
[4] A. Elsakka, U. Johannsen, O. Iupikov, M. N. Johansson, M. Ivashina, and A. B. Smolders, "A design concept of power efficient, high gain antenna system for mm-waves base stations," in *Proc. 15th Eur. Conf. Antennas Propag. (EuCAP)*, Mar. 2021, pp. 1–3.
[5] M. Fozooni, H. Q. Ngo, M. Matthaiou, S. Jin, and G. C. Alexandropoulos, "Hybrid processing design for multipair massive MIMO relaying with channel spatial correlation," *IEEE Trans. Commun.*, vol. 67, no. 1, pp. 107–123, Jan. 2019.
[6] T. A. H. Bressner, A. Farsaei, M. Fozooni, U. Johannsen, M. N. Johansson, and A. B. Smolders, "MIMO performance evaluation of isotropic, directional and highly-directional antenna systems for mm-wave communications," in *13th Eur. Conf. Antennas Propag. (EuCAP)*, May 2019, pp. 1–5.
[7] S. Jaeckel, L. Raschkowski, K. Börner, and L. Thiele, "QuaDRiGa: A 3-D multi-cell channel model with time evolution for enabling virtual field trials," *IEEE Trans. Antennas Propag.*, vol. 62, no. 6, pp. 3242–3256, Jun. 2014.
[8] *5G;NR; User Equipment (UE) Conformance Specification; Radio Transmission and Reception; Part 3: Range 1 and Range 2 Interworking Operation with other Radios*, document TR 38 521-3 V15.1.0, 3GPP, Paris, France, Apr. 2019.
[9] *User Equipment (UE) Radio Transmission and Reception*, document TS 138 101-2 V15.2.0, 3GPP, Paris, France, Jul. 2018.
[10] K. Kurokawa, "Power waves and the scattering matrix," *IEEE Trans. Microw. Theory Techn.*, vol. MTT-13, no. 2, pp. 194–202, Mar. 1965. [Online]. Available: http://ieeexplore.ieee.org/document/1125964/
[11] P.-S. Kildal, *Foundation Antenna Engineering: A Unified Approach for Line-of-Sight Multipath*, 3rd ed. Hoboken, NJ, USA: Artech House, 2015.
[12] S. F. Gregson, J. McCormick, and C. Parini, *Principles of Planar Near-Field Antenna Measurements* (IET Electromagnetic Waves), vol. 53. London, U.K.: Institution of Engineering and Technology, 2007.

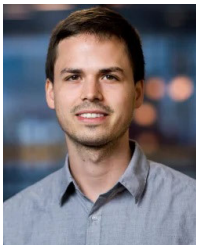

THOMAS A. H. BRESSNER received the B.S. degree in electrical engineering and information technology from Karlsruhe Institute of Technology (KIT), Germany, in 2012, the M.S. degree in electrical engineering from the KTH Royal Institute of Technology, Stockholm, Sweden, in 2015, the M.S. degree in electronic engineering from the Politecnico di Torino (POLITO), Italy, in 2015, and the M.S. degree in electrical engineering with a specialization in radio frequencies from Karlsruhe Institute of Technology (KIT), in 2016. He is currently pursuing the Ph.D. degree with the Department of Electrical Engineering, Eindhoven University of Technology (TUE). He contributes by his work on energy-efficient base stations for mobile communications to the European Project SILIKA.

AMR ELSAKKA received the B.Sc. degree in electronics and communications engineering from Cairo University, in 2008, the Postgraduate Diploma degree in telecommunications and information engineering from the National Telecommunications Institute, Egypt, in 2014, and the M.Sc. degree in radio science and engineering from Aalto University, Finland, in 2016. He is currently pursuing the dual Ph.D. degree with Eindhoven University of Technology, The Netherlands, and Chalmers University of Technology, Sweden. From 2010 to 2014, he worked as an Automation Engineer with Invensys (Schneider Electric), Cairo, Egypt. He was a Former Visiting Researcher at Ericsson AB, Sweden. His current research interest includes focal plane array antennas at mm-waves for mobile base stations applications.

AMIRASHKAN FARSAEI was born in Tehran, in 1991. He received the B.Sc. and M.Sc. degrees in electrical engineering from Sharif University of Technology, Tehran, Iran, in 2013 and 2015, respectively, and the Ph.D. degree from Eindhoven University of Technology, in 2021. During his Ph.D., he was a Visiting Researcher at Ericsson Research, for more than two years. He is currently a Researcher at IMEC. His research interests include signal processing and wireless communication.

MARTIN N. JOHANSSON (Senior Member, IEEE) received the M.S. degree in engineering physics and the Ph.D. degree in electromagnetics from Chalmers University of Technology, Gothenburg, Sweden, in 1986 and 1997, respectively. From 1987 to 1992, he was with Ericsson Radar Electronics AB, Mölndal, Sweden, designing antenna systems for airborne and satellite applications. In 1991, he worked with Cirrus Consulting AB, Gothenburg, on the design of the Arecibo radio telescope dual-reflector feed. He joined Ericsson Research at Ericsson AB, Gothenburg, in 1997, where he currently serves as an Expert in antenna technology. His current research interests include antenna technology for mobile communications, antenna system modeling, and deterministic propagation modeling.

OLEG A. IUPIKOV (Member, IEEE) received the M.Sc. degree *(cum laude)* in electrical engineering from Sevastopol National Technical University, Ukraine, in 2006, and the Ph.D. degree from Chalmers University of Technology, Gothenburg, Sweden, in 2017.

After graduating, he was working at Radio Engineering Bureau, Sevastopol. During this period, he was also a Visiting Researcher at the Netherlands Institute for Radio Astronomy (ASTRON), where he was involved in the development of the focal plane array simulation software for the APERTIF radio telescope. This visit was funded by the SKADS Marie Curie Visitor Grant and the APERTIF Project. He currently works as a Researcher with Chalmers University of Technology. He has authored/coauthored over 38 journal articles and conference papers. His research interests include receiving antenna array systems, in particular focal plane arrays for radio astronomy and microwave remote sensing applications, numerical methods for their analysis and optimization, signal processing algorithms for antenna systems, and integration of antennas with active components.

ROB MAASKANT (Senior Member, IEEE) received the M.Sc. and Ph.D. degrees *(cum laude)* in electrical engineering from Eindhoven University of Technology (TU/e), Eindhoven, The Netherlands, in 2003 and 2010, respectively.

He was employed as an Antenna Researcher at the Netherlands Institute for Radio Astronomy (ASTRON), Dwingeloo, The Netherlands, from 2002 to 2010. Since 2010, he has been with the Antenna Group of the Department of Electrical Engineering, Chalmers University of Technology (Sweden), where he held a postdoctoral position and an Assistant Professor. He is currently an Associate Professor with Chalmers University of Technology and TU/e. The latter position is owing to a five-year Vidi Grant from the Dutch research Council. He is the primary author of the CAESAR software, an advanced integral-equation based solver for the analysis of large antenna array systems. His current research interest includes the analysis and design of integrated antenna array systems for future wireless applications. He has served the AP Community as an Associate Editor for both the IEEE TRANSACTIONS ON ANTENNAS AND PROPAGATION and the IEEE ANTENNAS AND WIRELESS PROPAGATION LETTERS. He is in the Editorial Board of a unique open-access journal, namely *Forum for Electromagnetic Research Methods and Application Technologies* (FERMAT, http://www.e-fermat.org).

A. BART SMOLDERS (Senior Member, IEEE) was born in Hilvarenbeek, The Netherlands, in 1965. He received the M.Sc. and Ph.D. degrees in electrical engineering from Eindhoven University of Technology (TU/e), in 1989 and 1994, respectively.

From 1989 to 1991, he worked as an IC Designer at FEL-TNO, The Hague. From 1994 to 1997, he was a Radar System Designer with Thales, The Netherlands. From 1997 to 2000, he was the Project Leader of the Square Kilometer Array (SKA) with the Netherlands Foundation for Research in Astronomy (ASTRON). From 2000 to 2010, he was with NXP (formerly Philips) Semiconductors, The Netherlands, responsible for the innovation in the RF business line. Since 2010, he has been a full-time Professor with the Electromagnetics Group, TU/e, with special interest in antenna systems and applications. Next to his research activities, he is the Dean of the Department of Electrical Engineering, TU/e. He currently leads several research projects in the area of integrated antenna systems operating at frequencies up to 120 GHz for several application domains, including 5G/6G wireless communications, radar sensors, and radio-astronomy. He has published more than 150 papers.

Dr. Smolders is a Board Member of the Stichting Wetenschappelijke Activiteiten van het Nederlands (SWAN) URSI Committee and a member of the Advisory Board of ASTRON. He is the Junior Past Chairman of the IEEE Benelux Section and the Past Chair of the Nederlands Radio-en Elektronica Genootschap (NERG).

ULF JOHANNSEN (Member, IEEE) received the Dipl.-Ing. degree in communications engineering from Hamburg University of Technology (TUHH), Germany, in 2009, and the Ph.D. degree in electrical engineering from Eindhoven University of Technology (TU/e), The Netherlands, in 2013.

From 2013 to 2016, he worked as a Senior Systems Engineer at ATLAS ELEKTRONIK GmbH (Bremen, Germany), where his role was a System Designer and an Engineering Manager on autonomous underwater vehicle (AUV) systems with sonar payloads. In 2016, he was appointed as an Assistant Professor with the Electromagnetics Group, Department of Electrical Engineering, TU/e. His research interests include millimeter-wave antenna systems and antenna integration. He is a member of VDE and the Chairperson of the IEEE Benelux Joint AP/MTT Chapter.